

LONG CONTEXT COMPRESSION WITH ACTIVATION BEACON

Anonymous authors

Paper under double-blind review

ABSTRACT

Long context compression is a critical research problem due to its significance in reducing the high computational and memory costs associated with LLMs. In this paper, we propose Activation Beacon, a plug-in module for transformer-based LLMs that targets effective, efficient, and flexible compression of long contexts. To achieve this, our method introduces the following technical designs. 1) We directly compress the activations (i.e. keys and values at every layer), rather than leveraging soft prompts to relay information (which constitute a major bottleneck to encapsulate the complex information within long contexts). 2) We tailor the compression workflow, where each fine-grained input unit is progressively compressed, enabling high-quality compression and efficient computation during both training and inference. 3) We train the model through compression-based auto-regression, making full use of plain texts and instructional data to optimize the model’s compression performance. 4) During training, we randomly sample a compression ratio at each step, teaching the model to support a wide range of compression configurations. Extensive evaluations are conducted on various long-context tasks whose lengths (e.g., 128K) may far exceed the maximum training length (20K), such as document understanding, few-shot learning, and Needle-in-a-Haystack. Whilst existing methods struggle to handle these challenging tasks, Activation Beacon maintains a comparable performance to the uncompressed baseline across various scenarios, achieving a 2x acceleration in inference time and an 8x reduction of memory costs for KV cache.

1 INTRODUCTION

Large language models (LLMs) need to process long contexts to accomplish many important tasks, such as long-document understanding (Jiang et al., 2024b), long-content creation (Bai et al., 2024), and long-term memorization/reasoning (Zhang et al., 2024). To address these needs, modern LLMs are built with extended context windows (e.g., 128K) that enable remarkable long-context processing capabilities (OpenAI et al., 2024; Yang et al., 2024; Dubey et al., 2024). Despite their effectiveness, LLMs encounter *efficiency challenges* in processing long contexts. On one hand, transformer-based LLMs incur substantial computational costs due to the quadratic complexity of self attention. On the other hand, they require tremendous GPU memory to hold the KV cache of the entire sequence for faster decoding. Both computation and memory costs increase as the context length grows.

A wide array of studies are dedicated to alleviating efficiency issues, among which context compression is a promising direction (Mu et al., 2023; Chevalier et al., 2023; Ge et al., 2024; Jiang et al., 2023a;b). This approach aims to compress raw input into more concise representations, allowing the generation process to be conditioned on a shorter context. Therefore, it helps to reduce both computation cost of inference and memory cost from KV cache, while also enabling the processing of longer inputs than the LLM’s built-in context window.

Despite the current progresses, it remains a tough challenge to compress long contexts. Specifically, existing methods usually summarize the context into a few soft tokens (Chevalier et al., 2023; Ge et al., 2024), which constitute the major bottleneck to summarize the complex information within long contexts. Besides, they try to compress the context “all-at-once”, lacking a fine-grained handling of the detailed information. Moreover, these soft tokens must be re-encoded before generation, resulting in inferior efficiency in both training and inference. Lastly, these methods are learned to compress with a fixed number of soft tokens, thus, it’s hard to customize the compression ratio for downstream tasks. While some alternative methods focus on deleting unimportant tokens (Jiang

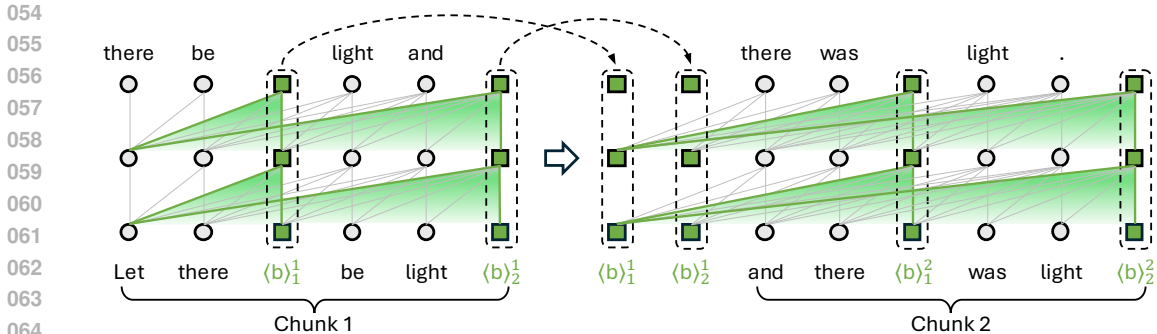


Figure 1: Overview of Activation Beacon. The context is partitioned into chunks. Each chunk is further split into fine-grained units and interleaved with beacon tokens according to a compression ratio (2 in the figure). The LLM encodes one chunk at a time, compressing the context into beacon tokens’ activations, which are *accumulated* and *reused* for encoding following chunks.

et al., 2023b; Li et al., 2024b), they depend on the input question to estimate the token importance, limiting their efficiency in real-world multi-turn scenarios.

To address the above challenges, we present Activation Beacon (Figure 1), a plug-in module to transformer-based LLMs that enables effective, efficient, and flexible compression of long contexts. Activation Beacon is featured with the following technical designs.

First of all, we introduce a new special token, called the beacon token $\langle b \rangle$. The context is distilled into beacon tokens’ *activations* (i.e. keys and values at every layer), whose capacity are large enough to encapsulate the complex information within long contexts.

Next, we tailor the compression workflow, where each fine-grained context unit is progressively compressed. Specifically, the long context is partitioned into equal-size chunks. Each chunk is further split into fine-grained units of size α where α is the desired compression ratio. A group of beacon tokens are interleaved with these units (one beacon token is dispatched to the end of every unit). The LLM encodes one chunk at a time, distilling the chunk’s information into beacon tokens’ activations during self attention. After encoding, the raw tokens’ activations are *discarded*; while the beacon tokens’ activations are *accumulated* and *reused* for encoding following chunks. This progressive workflow brings forth several advantages: 1) It can handle inputs longer than the backbone LLM’s context window as the chunk size is small. 2) It achieves fine-grained compression since the attention scope of each beacon token is differentiated. 3) By caching and reusing activations, it facilitates contiguous gradient propagation in training, avoids re-encoding overhead in inference, and allows for incrementally updating the compression results in multi-turn scenarios.

Finally, Activation Beacon is learned with compression-based auto-regression to optimize the generation quality conditioned on the compressed context. Thanks to high sample efficiency, the model can be effectively trained with 1B plain corpus and 30K fine-tuning samples (maximum context length is 20K), which can be quickly accomplished. During training, we randomly sample the compression ratio for each chunk, enhancing the model’s flexibility to tackle different compression ratios in downstream tasks. Note that all beacon tokens share the same token embedding, one can use arbitrary number of beacon tokens to achieve the desired compression ratio by repeating.

In our experiments, Activation Beacon is applied to Llama-2 (Touvron et al., 2023) and Qwen-2 (Yang et al., 2024). We evaluate the resulted models on a variety of long-context tasks (whose lengths may be much longer than the training length, e.g., 128K), such as document understanding, few-shot learning, and Needle-in-a-Haystack. Whilst existing methods struggle to handle these challenging tasks, Activation Beacon maintains a comparable performance to the uncompressed baseline across various compression configurations, meanwhile achieving 2x acceleration and 8x KV cache reduction. Moreover, the LLM’s original capabilities on short context is well preserved.

2 RELATED WORKS

Recently, processing long context has become a fundamental capability of modern LLMs (OpenAI et al., 2024; Dubey et al., 2024; Yang et al., 2024; DeepSeek-AI, 2024). The recipe of context window extension is roughly the same: modifying the rotary position embedding (Su et al., 2021)

108 by extrapolation and interpolation (Chen et al., 2023a; ntk, 2023; Peng et al., 2023; Ding et al.,
109 2024), and leveraging long-dependency data in both the pre-training and post-training stage. Despite
110 the impressive progress in effectiveness, LLMs face significant challenges in efficiency. There is
111 significant computational cost due to the quadratic complexity of transformer, and huge memory cost
112 because LLMs need to hold the KV activations of the entire sequence on GPU for faster decoding.
113 Multiple threads of research endeavour to reduce these costs, which are discussed as follows.

114 **Sparse Attention.** Conventional sparse attention methods require re-training a model from scratch
115 using the designated sparse patterns (Zaheer et al., 2020; Beltagy et al., 2020). However, extensive
116 recent studies have identified that the attention pattern of LLMs are naturally sparse despite they are
117 densely trained (Jiang et al., 2024a; Xiao et al., 2023; Han et al., 2023; Zhu et al., 2024). They also
118 propose to dynamically set appropriate sparse patterns for each head so that the attention mass can be
119 largely preserved, leading to competitive performance against the full-attention method with reduced
120 computation. However, these methods require holding all KV activations on chip to dynamically
121 determine the optimal sparse patterns, making them unsuitable for KV cache reduction. [There are
122 some sparse attention methods that directly evict the middle tokens \(Han et al., 2023; Xiao et al.,
123 2023\).](#) Despite their high efficiency and ability to generate endless fluent texts, these methods’
124 cannot memorize information in the middle contexts, leading to inferior performances on long-
125 context tasks [Xiao et al. \(2024\).](#)

126 **KV Compression.** This line of research focuses on compressing the KV activations to reduce
127 the attention computation as well as the cache size. Since the KV activations are per-layer, per-
128 head, per-token, and per-channel float numbers, they can be reduced from all the five dimensions
129 (including the numerical dimension). [For example, CLA \(Brandon et al., 2024\) shares the KV cache
130 across multiple layers; GQA \(Ainslie et al., 2023\) compresses multiple key/value heads into a single
131 one; MLA \(DeepSeek-AI, 2024\) compresses the channels into fewer and more compact ones; and
132 KIVI \(Zirui Liu et al., 2023\) quantizes the numerical value in the activations. The sequence-wise
133 compression \(also known as context compression\), where Activation Beacon falls, is introduced
134 in the following paragraph. It is orthogonal to the compression along other dimensions, and the
135 complementary effect of the compression along different dimension could be left for future work.
136 Besides, some recent studies design efficient strategies for offloading and transferring KV cache \(Liu
137 et al., 2023; Xiao et al., 2024\). They can also be jointly used with KV compression techniques to
138 achieve more efficient long-context generation.](#)

138 **Context Compression.** This type of methods aim to compress the raw context into shorter yet more
139 compact representations. Existing studies are usually tailored for compressing short context (less
140 than 1K), which tend to be sub-optimal for long-context compression. Specifically, Gisting (Mu
141 et al., 2023) compresses the user instruction into gist activations all at once. As a result, it cannot
142 process context longer than the backbone LLM’s window. CCM (Kim et al., 2024) extends Gisting to
143 compress conversations in online chatting, yet it cannot be used in general long context tasks such as
144 long document understanding. ICAE (Ge et al., 2024) and AutoCompressor (Chevalier et al., 2023)
145 alleviate this problem by segmenting the long context into chunks and compressing each chunk, in
146 order to compress contexts longer than the backbone LLM’s window. [CEPE \(Yen et al., 2024\) shares
147 a similar workflow while introducing a standalone encoder to compress the context and utilizing
148 the compression results through a cross-attention module.](#) However, these methods compress the
149 context into soft tokens, which are the major bottleneck to encapsulate the complex information in
150 long contexts. Their compression workflow also lacks fine-grained handling of the chunked inputs,
151 resulting in inferior compression quality. [Moreover, these methods must perform re-encoding or
152 employ additional cross-attention mechanism to utilize the compressed soft tokens, which introduces
153 extra overhead.](#) Lastly, since the number of soft tokens are pre-defined, it is hard to flexibly assign the
154 compression ratio for downstream tasks. Another branch of methods (Jiang et al., 2023b; Li et al.,
155 2024b) propose to delete unimportant tokens to realize compression. However, they depend on the
156 input question to accurately estimate the token importance, leading to low efficiency in real-world
157 multi-turn scenarios. Compared with existing approaches, Activation Beacon is able to achieve more
158 effective, efficient, and flexible compression. [Based on context compression techniques, there are
159 some innovated frameworks like LLoCO \(Tan et al., 2024\). It is built upon a compressor and a
160 decoder, where the context is compressed offline and offloaded into a retrieval system. The decoder
161 then efficiently responds to the user inputs based on retrieved compression results. Both modules are
learned with in-domain fine-tuning. Our work aims at improving the compressor itself, and hence is
orthogonal to these frameworking research.](#)

3 METHODOLOGY

LLMs accomplish arbitrary tasks in the form of next-token prediction. Formally, given the context $X = [x_1, \dots, x_n]$, the LLM generates the next token based on all preceding tokens and its well-trained parameters: $\Pr(x_{n+1} | x_1, \dots, x_n; \Theta)$. Transformer-based LLMs incur heavy computation cost due to the quadratic complexity of self attention; besides, they require tremendous GPU memory to store the KV cache of $x_{\leq n+1}$ for faster decoding (Zhang et al., 2023). Both the costs in computation and memory significantly expand when the context length increases.

Activation Beacon employs a new special token, namely beacon token $\langle b \rangle$, and condenses the raw context X into beacon tokens’ activations Ψ (i.e. their keys and values at every layer). The next-token prediction is converted to condition on the compressed context instead of the plain one. Given $|\Psi| < |X|$, both the computation cost and the KV cache size are reduced. Additionally, the LLM is enabled to handle context longer than its window size based on the compressed representations. We tailor the compression mechanism and the learning method of Activation Beacon towards achieving effective, efficient, and flexible compression, which will be elaborated in the following.

3.1 COMPRESSION MECHANISM

Overview. We propose to *progressively compress each fine-grained units of long contexts*. Specifically, given the input context X whose length may exceed the LLM’s context window N , it is first partitioned into chunks of the same size w (e.g., 1024):

$$[x_1, \dots, x_n] \xrightarrow{\text{Partition}} [X_1, \dots, X_{\lceil n/w \rceil}], X_i = [x_{(i-1)w+1}, \dots, x_{iw}]^1 = [x_1^i, \dots, x_w^i]. \quad (1)$$

Next, for each chunk X_i , we determine a compression ratio α_i (w is evenly divisible by α_i). The chunk is further split into fine-grained units of size α . Then a group of $k_i = w/\alpha_i$ beacon tokens, $B_i = [\langle b \rangle_1^i, \dots, \langle b \rangle_{k_i}^i]$, are *interleaved* with these units. In other words, one beacon token is dispatched to the end of every unit:

$$X_i \xrightarrow{\text{Interleave } B_i} X_i' = [x_1^i, \dots, x_{\alpha_i}^i, \langle b \rangle_1^i, \dots, x_{w-\alpha_i+1}^i, \dots, x_w^i, \langle b \rangle_{k_i}^i]. \quad (2)$$

The LLM encodes these chunks *one by one*, compressing the contextual information of each chunk into the corresponding beacon tokens’ activations during self attention. After encoding X_i' , we *discard* activations of all the raw tokens X_i , while we *accumulate* the activations of the beacon tokens B_i . When encoding the next chunk X_{i+1}' , the LLM directly conditions on the accumulated beacon activations as a proxy to the raw context $X_{\leq i}$.

This progressive workflow benefits both compression quality and running efficiency. On one hand, it enables thorough distillation of complex information within long contexts and allows for the compression of inputs that exceed the LLM’s context window. On the other hand, by caching and reusing beacon tokens’ activations, it avoids redundant computation and allows for incrementally update of the compression results in multi-turn interactions.

Encoding and Compression. As shown in Figure 2, Activation Beacon reuses all modules of the LLM except imposing a slight modification on self attention. Without loss of generality, for the i -th chunk X_i' , the encoding process can be written as:

$$\text{LLM}(\underbrace{\langle b \rangle_1^i, \dots, \langle b \rangle_{k_i-1}^i}_{\text{beacon activations accumulated from } X_{<i}'} \underbrace{x_1^i, \dots, x_{\alpha_i}^i, \langle b \rangle_1^i, \dots, x_{w-\alpha_i+1}^i, \dots, x_w^i, \langle b \rangle_{k_i}^i}_{\text{the current chunk } X_i'}), \quad (3)$$

where the input to the LLM is a mix of the activations accumulated from previous chunks and the tokens to be encoded within the current chunk. Let D denote the LLM’s hidden size, $\mathbf{H} \in \mathbb{R}^{(w+k_i) \times D}$ denote input hidden states to self attention in an arbitrary layer of the LLM. We first slice out the hidden states of raw tokens and beacon tokens:

$$\mathbb{I}^r = \{j | x_j^i \neq \langle b \rangle\}, \quad \mathbb{I}^b = \{j | x_j^i = \langle b \rangle\}; \quad \mathbf{H}^r = \mathbf{H}[\mathbb{I}^r], \quad \mathbf{H}^b = \mathbf{H}[\mathbb{I}^b]. \quad (4)$$

Then the hidden states are projected into queries, keys, and values:

$$\begin{aligned} \mathbf{Q}^r &= \mathbf{W}_Q^r \mathbf{H}^r, & \mathbf{K}^r &= \mathbf{W}_K^r \mathbf{H}^r, & \mathbf{V}^r &= \mathbf{W}_V^r \mathbf{H}^r, \\ \mathbf{Q}^b &= \mathbf{W}_Q^b \mathbf{H}^b, & \mathbf{K}^b &= \mathbf{W}_K^b \mathbf{H}^b, & \mathbf{V}^b &= \mathbf{W}_V^b \mathbf{H}^b, \end{aligned} \quad (5)$$

¹The last chunk $X_{\lceil t/w \rceil}$ may be shorter than w , which is omitted for simplicity.

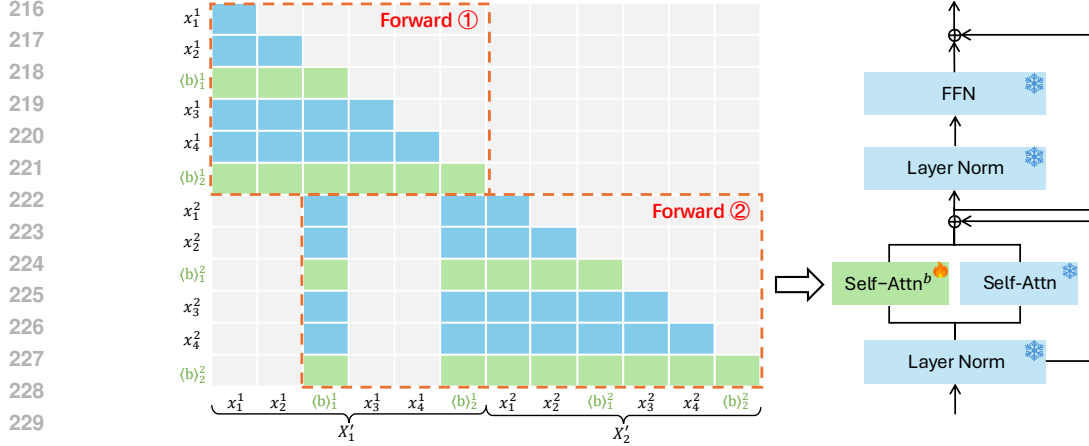


Figure 2: Activation Beacon performs compression during self attention while reusing all other modules of the LLM. *Forward ①*: encode and compress the first chunk. *Forward ②*: encode and compress the second chunk conditioned on activations of preceding beacon tokens.

where \mathbf{W}_*^r are the LLM’s original projection matrices and \mathbf{W}_*^b are the newly introduced matrices to handle beacon tokens only. Afterwards, the query/key/value states of raw tokens and beacon tokens are scattered back to acquire $\mathbf{Q}, \mathbf{K}, \mathbf{V} \in \mathbb{R}^{(w+k_i) \times D}$:

$$\mathbf{Q}[\mathbb{I}^r] = \mathbf{Q}^r, \mathbf{Q}[\mathbb{I}^b] = \mathbf{Q}^b; \quad \mathbf{K}[\mathbb{I}^r] = \mathbf{K}^r, \mathbf{K}[\mathbb{I}^b] = \mathbf{K}^b; \quad \mathbf{V}[\mathbb{I}^r] = \mathbf{V}^r, \mathbf{V}[\mathbb{I}^b] = \mathbf{V}^b. \quad (6)$$

Finally, the standard self-attention is computed over the entire input:

$$\mathbf{A} = \text{softmax} \left(\text{mask} \left(\frac{\mathbf{Q} \{ \mathbf{K}^{ac}; \mathbf{K} \}^T}{\sqrt{D}} \right) \right), \quad \mathbf{V} = \mathbf{A} \{ \mathbf{V}^{ac}; \mathbf{V} \}. \quad (7)$$

In the above equations, $\{ \cdot ; \cdot \}$ denotes matrix concatenation. $\mathbf{K}^{ac}, \mathbf{V}^{ac} \in \mathbb{R}^{m_{i-1} \times D}$ are the beacon tokens’ activations accumulated from previous chunks where $m_{i-1} = \sum_{j=1}^{i-1} k_j$, and mask denotes the causal attention mask. During self attention, all tokens are encoded by their relative positions ($[m_{i-1}, \dots, m_i + w - 1]$ for queries and $[0, \dots, m_i + w - 1]$ for keys). The value states \mathbf{V} , are further processed by other modules (e.g., output projection, MLP, and LayerNorm) before passing to the next layer. After self attention, the keys and values of beacon tokens, i.e. \mathbf{K}^b and \mathbf{V}^b , have distilled the contextual information of X_i . They are incrementally accumulated:

$$\mathbf{K}^{ac} = \{ \mathbf{K}^{ac}; \mathbf{K}^b \}, \quad \mathbf{V}^{ac} = \{ \mathbf{V}^{ac}; \mathbf{V}^b \}. \quad (8)$$

In our default setting, the beacon tokens are interleaved with raw tokens. This leads to a differentiated attention scope for each beacon token ($(b)_j^i$ attends to one more interval than $(b)_{j-1}^i$), contributing to the *fine-grained* compression of the context. We also explore the setting to dispatch all beacon tokens at the end of the chunk, which results in inferior compression quality (§4.6).

Note that unlike ICAE (Ge et al., 2024) and LLMLingua (Jiang et al., 2023b), Activation Beacon unifies generation and compression operations within a single forward pass of the LLM. That is to say, the hidden states of the last input token $\mathbf{H}[\mathbb{R}^r[-1]]$ is directly used to decode the next token without resorting to another decoder model.

Efficiency Analysis. Activation Beacon reduces the KV cache by α times where α is the *average compression ratio* and hence the memory cost. This is because it only needs to store the compressed activations of the preceding chunks instead of the raw activations. In terms of computation, the situation is a bit more complex. Specifically, Activation Beacon significantly reduces the computation in self attention, because each token only needs to interact with local tokens within the chunk and preceding beacon tokens, which are approximately α times shorter than the raw context. However, it also triggers more computation to encode the inserted beacon tokens in other modules (e.g., MLP). Formally, given an LLM with a fixed number of layers, attention heads, and hidden size, let s denote the input context length, s^{pst} denote the cached context length, the forward FLOPs is:

$$\text{FLOPs} = F^{Att}(s, s^{pst}) + F^{Oth}(s), \quad (9)$$

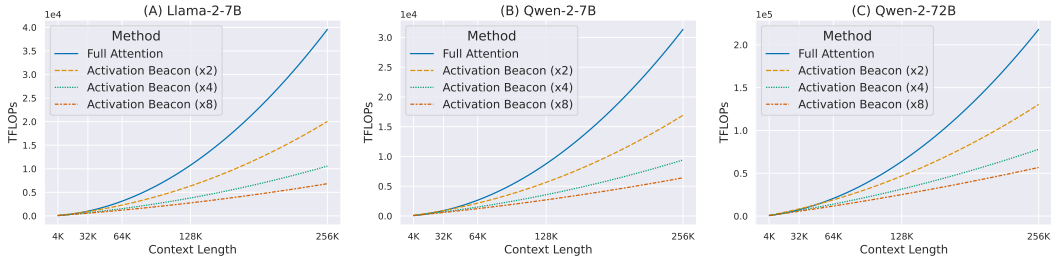


Figure 3: Comparison of the forward FLOPs of different models using full attention and Activation Beacon (the compression ratio is annotated in the brackets).

where F^{Att} is the computation during self attention, and F^{Oth} is the computation of other modules. For full-attention models, $s = n, s^{pst} = 0$. For “beaconed” models, the FLOPs is:

$$FLOPs^{bcn} = \sum_{i=1}^{\lceil \frac{n}{w} \rceil} F^{Att} \left(\frac{(\alpha + 1)w}{\alpha}, \frac{(i - 1)w}{\alpha} \right) + F^{Oth} \left(n + \lceil \frac{n}{\alpha} \rceil \right). \quad (10)$$

Since the implementation of F^{Att} and F^{Oth} depends on the actual setting of the LLM (see Appendix B), we visualize the FLOPs curve of three different LLMs in Figure 3. It can be observed that Activation Beacon consistently saves computational costs across different model settings and scales. The extent of saving amplifies as the context length grows, finally achieving more than x4 reduction at 256K context. The specific implication on latency is studied in §4.3.

3.2 LEARNING METHOD

Compression-Based Auto-Regression. Activation Beacon is learned to optimize the generation quality conditioned on the mixture of the compressed context and the local context. Formally, the compression-based next-token prediction loss is minimized:

$$\min_{\Theta^b} \sum_{i=2}^{\lceil N/w \rceil} \sum_{j=1}^w \Pr(x_j^i \mid \langle b \rangle_1^1, \dots, \langle b \rangle_{k_{i-1}}^{i-1}, x_1^i, \dots, x_{j-1}^i; \Theta, \Theta^b). \quad (11)$$

Θ denotes the parameters of the LLM itself, which are *fixed* throughout the training process. Θ^b includes the projection matrices for beacon tokens at each layer W_Q^b, W_K^b, W_V^b , and the token embedding of beacon token $e_{(b)}$ (we use one *shared* embedding for all beacon tokens). The training loss can be obtained from all tokens except the ones in the first chunk. Such a property leads to high sample efficiency that maximizes the use of training data. Note that we exclude the beacon tokens from the above loss (setting their labels to -100) because they are solely intended for compression.

No Stop Gradients. Recurrent memory methods (Chevalier et al., 2023; Bulatov et al., 2023) stop the gradients back-propagation at a given chunk number to improve the training efficiency. This is because these methods depend on the *final-layer* outputs of preceding chunks to encode the current chunk, which results in deepened computation graph as more chunks are involved. In contrast, Activation Beacon only depends on the *previous-layer* outputs of preceding chunks (the encoding of X_i^l at layer l only conditions on the results of X_{i-1}^l at layer $l - 1$), which is the same as any auto-regressive LLMs. Thus, the gradients can naturally flow through all chunks to optimize the compression effect over long contexts.

Chunk-Wise Random Compression Ratio. To teach the model to flexibly support diverse compression granularities, the compression ratio α_i for the i -th chunk is *randomly sampled* from $\{2, 4, 8, 16, 32\}$ during training. At inference, one can choose one compression ratio according to the specific efficiency requirement in downstream tasks and stick to it for all chunks.

4 EXPERIMENTS

Our experiment mainly study Activation Beacon’s effectiveness (§4.2), efficiency (§4.3), and flexibility (§4.4) in long context compression. Besides, we explore Activation Beacon’s impact on short-context capabilities of the backbone LLM (§4.5) and the effect of each technical design (§4.6).

Table 1: Evaluation on LongBench (Bai et al., 2023). Activation Beacon maintains comparable performance to the uncompressed baseline (Full-FT), outperforming other compression methods. “Length” indicates the number of tokens in the *input* context.

| Model | Method | Length | Single-Doc | Multi-Doc | Summ. | Few-Shot | Code |
|------------|------------|-------------|-------------|-------------|-------------|-------------|-------------|
| Llama-2-7B | Full | 4K | 24.7 | 22.4 | 24.6 | 63.2 | 57.7 |
| | Full-FT | 32K | 34.8 | 27.5 | 23.2 | 61.8 | 57.8 |
| | AutoCompr. | 32K | 12.9 | 16.4 | 16.3 | 23.8 | 39.4 |
| | ICAE | 32K | 19.5 | 19.2 | 19.5 | 24.8 | 27.8 |
| | LongLLML. | 32K | 21.5 | 18.8 | 21.7 | 49.5 | 53.2 |
| | SnapKV | 4K | 24.2 | 22.6 | 16.3 | 60.1 | 57.7 |
| Ours | 32K | 34.9 | 27.5 | 25.0 | 61.4 | 57.8 | |
| Qwen-2-7B | Full | 32K | 38.8 | 37.5 | 26.7 | 70.1 | 60.3 |
| | Full-FT | 32K | 41.0 | 40.6 | 26.8 | 68.5 | 66.1 |
| | LongLLML. | 32K | 24.7 | 20.3 | 26.3 | 55.9 | 50.1 |
| | SnapKV | 32K | 38.7 | 37.6 | 26.2 | 67.1 | 60.3 |
| | Ours | 32K | 40.5 | 40.3 | 26.8 | 68.4 | 66.4 |

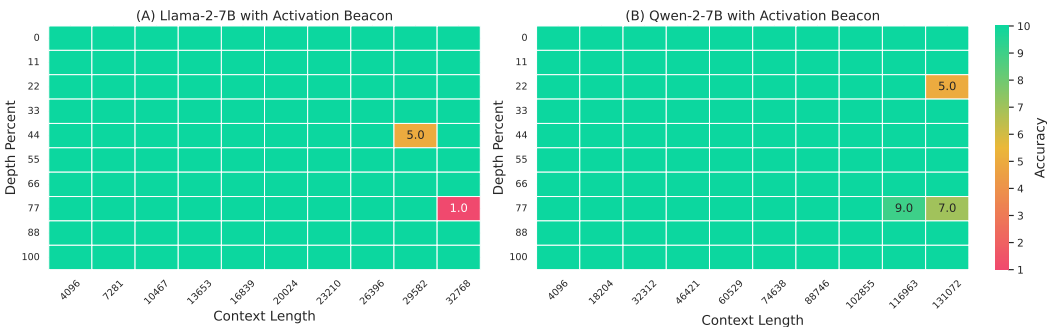


Figure 4: Evaluation on Needle-in-a-Haystack. Activation Beacon can accurately retrieve the needle most of the time, despite the context is far longer than its training data.

4.1 SETTINGS

Implementation. Activation Beacon is applied to Llama-2-7B (chat)² and Qwen-2-7B (instruct). The chunk size w is 1024 for Llama-2 and 2048 for Qwen-2. FlashAttention-2 (Dao, 2023) is used to speed up attention computation. For all our experiments, we use Huggingface framework (Wolf et al., 2020) and one 8xA800 (80G) machine.

Training. The training consists of two phases. In pre-training, we use 1B tokens sampled from RedPajama (Computer, 2023). The eos token is appended to the end of every document. In fine-tuning, we leverage LongAlpaca (Chen et al., 2023b), BookSum (Kryściński et al., 2022), and synthetic data from GPT-3.5 (details in Appendix A). All the training samples are shorter than 20K. The batch size is 8. The learning rate is 5e-5 for pre-training and 1e-5 for fine-tuning, with linear decay and no warmup. As introduced, the LLM’s original parameters are frozen throughout the training process.

Baselines. We compare Activation Beacon with the uncompressed baseline (denoted as Full) and the uncompressed baseline fine-tuned with the same training data (denoted as Full-FT). Besides, we include the following context compression methods that can tackle long context for comparison, including AutoCompressors (Chevalier et al., 2023), ICAE (Ge et al., 2024), LongLLMLingua (Jiang et al., 2023b), and SnapKV (Li et al., 2024b). The first two methods only support Llama-2. To guarantee fair comparison, we fine-tune their official checkpoints using the same training data.

4.2 COMPRESSION EFFECTIVENESS

To verify the compression effectiveness of Activation Beacon, we evaluate it on LongBench (Bai et al., 2023), which consists of a variety of long-context tasks with 32K maximum length, including

²We use Llama-2 because AutoCompressor and ICAE are based on it, both of which are important baselines.

Table 2: Evaluation on Multi-Needle-in-a-Haystack where the questions are issued one-by-one in a multi-turn conversation setting. All compression methods use a x8 compression ratio. Activation Beacon consistently outperforms other compression baselines while enjoying lower latency, especially when the context lengthens and the turn number increases.

| Model | Length | Method | 1-Turn | | 2-Turn | | 3-Turn | |
|------------|--------|------------|-------------|--------------|-------------|--------------|-------------|--------------|
| | | | Acc | Latency | Acc | Latency | Acc | Latency |
| Llama-2-7B | 32K | Full-FT | 9.75 | 1.336 | 9.45 | 1.532 | 9.10 | 1.726 |
| | | AutoCompr. | 1.60 | 2.135 | 1.50 | 2.561 | 1.50 | 2.994 |
| | | ICAE | 2.15 | 1.182 | 2.15 | 1.476 | 2.00 | 1.805 |
| | | LongLLML. | 2.05 | 2.813 | 2.00 | 5.062 | 2.00 | 7.034 |
| | | SnapKV | 1.00 | 0.859 | 1.00 | 1.656 | 1.00 | 2.199 |
| | | Ours | 9.75 | 1.153 | 9.40 | 1.356 | 9.05 | 1.638 |
| Qwen-2-7B | 128K | Full-FT | 9.75 | 4.399 | 9.50 | 5.254 | 9.20 | 6.153 |
| | | LongLLML. | 2.00 | 10.455 | 1.55 | 19.768 | 1.50 | 27.751 |
| | | SnapKV | 9.45 | 3.955 | 8.95 | 7.803 | 8.85 | 10.659 |
| | | Ours | 9.70 | 2.445 | 9.35 | 2.773 | 9.10 | 2.981 |

question answering, summarization, few-shot learning, and code completion. Since Llama-2 has a context window of 4K, we truncate the context longer than 4K from middle before inputting to it. For compression methods implemented on Llama-2, we set *adaptive* compression ratio, translating to x2 compression for 4K-8K contexts, x4 compression for 8K-16K contexts, and x8 compression for 16K-32K contexts. For methods implemented on Qwen-2, we apply a uniform compression ratio of x4. The results are reported in Table 1. We highlight two observations in the following.

Firstly, **Activation Beacon achieves superior compression quality over other compression baselines across all tasks.** Concretely, it significantly outperforms ICAE and AutoCompressor, which verifies that several soft tokens are not enough to encapsulate the rich information within long contexts. LongLLMLingua also lags far behind Activation Beacon because it needs to delete too many tokens given a high compression ratio (e.g., x4, x8), which may destroy the coherence of the context and lose important information. Despite SnapKV’s top performance among baselines, it cannot compress context longer than the backbone LLM’s window. This is because it estimates the token importance based on self attention, which becomes inaccurate once the context exceeds the window size, limiting its practical usage when compressing long contexts.

Secondly, **Activation Beacon achieves comparable performance to the fine-tuned uncompressed baseline (Full-FT)** even though Full-FT takes in the entire context without compression. This indicates that Activation Beacon is able to compress long contexts without evident information loss, which validates its high compression quality yielded from the progressive compression workflow. Furthermore, Activation Beacon improves upon Llama-2 by a large margin despite their context window is the same, i.e. 4K. The gain is because Llama-2 (Full) directly uses the truncated 4K context, while Activation Beacon compresses the 32K context into 4K compact activations. This implies that Activation Beacon can effectively introduce useful information from Llama-2’s unseen context. Therefore, it can be viewed as an efficient approach for context extension.

We further evaluate Activation Beacon on Needle-in-a-Haystack (NIAH) following the official settings (gkamradt, 2023) to investigate whether it will lose fine-grained information. The accuracy is estimated by ChatGPT (ranges from 1 to 10). For both Llama-2 and Qwen-2, we set adaptive compression ratio as introduced above. The results are shown in Figure 4. It can be observed that Activation Beacon **precisely retrieves the needle** most of the time. Note that Activation Beacon conducts *query-independent* compression, which means it has no prior knowledge of what to compress and what not. Hence, this remarkable performance again validates our tailored compression mechanism and learning method can preserve the fine-grained contextual information. Moreover, Activation Beacon is only trained on context shorter than 20K, while its compression capability can generalize to far longer contexts (e.g., 128K).

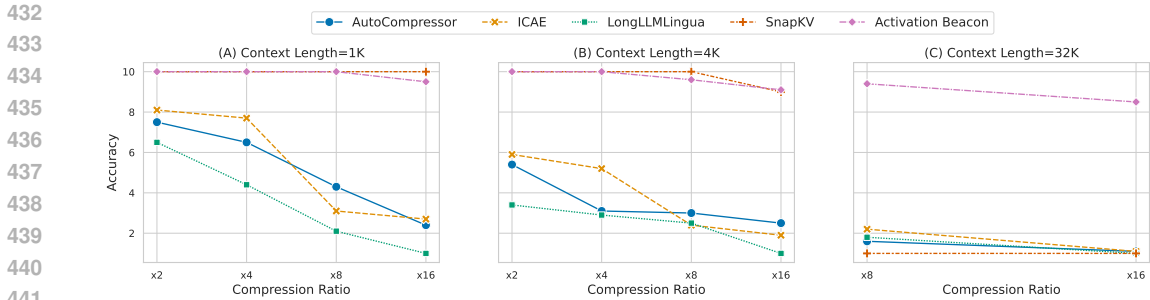


Figure 5: Evaluation on Needle-in-a-Haystack with various compression ratios based on Llama-2. Activation Beacon achieves top compression quality across all compression configurations.

4.3 COMPRESSION EFFICIENCY

We evaluate the efficiency of Activation Beacon based on the Multi-Needle-in-a-Haystack task following NeedleBench (Li et al., 2024a). Specifically, we fix the context length to 32K for Llama-2 and 128K for Qwen-2, and insert 3 different needles at different positions. The task is organized in a multi-turn conversation setting, where the model is asked to retrieve one specific needle in each turn. The experiment is repeated 20 times for each model with distinct needle positions. In Table 2, we report the accuracy and the end-to-end latency of compression & generation (measured in seconds).

It can be observed that **Activation Beacon enjoys lower latency than other compression baselines**. Notably, it is 1.8x faster than AutoCompressor because it does not have to re-encode the soft tokens from previous chunks. It also leads to 9.3x and 3.6x acceleration upon LongLLMLingua and SnapKV given three turns, respectively. This is because both baselines are query-dependent while Activation Beacon is not, which eliminates the need to re-compute the compression results for different input questions. Moreover, Activation Beacon demonstrates consistent speed-up over the Full-FT baseline, achieving **2x acceleration at 128K context length**. This matches our estimation in Figure 3(b) as Activation Beacon (x8) saves half of the computation. In the meanwhile, since the compression ratio is x8, it leads to **8x reduction of the KV cache**. Lastly, Activation Beacon always attains nearly-lossless generation quality against the uncompressed baseline, which is in line with previous observations.

4.4 COMPRESSION FLEXIBILITY

Activation Beacon is learned to support various compression ratios during training. In Figure 5, we evaluate its compression quality under different compression ratios and context lengths. According to the figure, Activation Beacon maintains top accuracy across all compression ratios, outperforming most compression baselines by a large margin. Though SnapKV performs on par with our method at 1K and 4K context length, it fails to compress inputs longer than the LLM’s window size, which may limit its practical usage. To summarize, Activation Beacon is a flexible solution to long context compression with the support of diverse compression ratios and various context lengths. Generally, we recommend to use x8 compression ratio as it preserves most information with high efficiency.

4.5 SHORT-CONTEXT CAPABILITIES

Since Activation Beacon interleaves beacon tokens with raw tokens and is primarily trained with long-context tasks, it is intriguing to examine whether the current recipe will impair the short-context capabilities of the backbone LLM. In Table 3, we compare Activation Beacon with the original LLM

Table 3: Activation Beacon preserves the short-context capabilities of the backbone LLM.

| Model | Method | MMLU | ARC-C | BoolQ | GSM8K |
|------------|--------|------|-------|-------|-------|
| Llama-2-7B | Full | 47.5 | 48.5 | 86.2 | 9.2 |
| | Ours | 46.6 | 48.4 | 86.5 | 9.3 |
| Qwen-2-7B | Full | 70.1 | 62.7 | 87.1 | 76.0 |
| | Ours | 69.1 | 62.7 | 87.2 | 76.2 |

(Full) on popular benchmarks, including MMLU (Hendrycks et al., 2021), ARC-Challenge (Bhaktavatsalam et al., 2021), BoolQ (Clark et al., 2019), and GSM8K (Cobbe et al., 2021). We can observe that Activation Beacon leads to very little performance degradation on short-context tasks.

In other words, the short-context capabilities are well preserved. We conjecture that the primary reason is the LLM’s original parameters are frozen throughout the training process.

4.6 ABLATION STUDIES

We study the impact of each technical factor, including the compression of fine-grained context units, the sampling strategy of compression ratio, and training stages. The experiments are based on Qwen-2-7B and Single-Doc QA task from LongBench (32K context with x4 compression ratio). The results are shown in Table 4. Firstly, instead of splitting the chunk into fine-grained units and interleaving beacon tokens, we append all beacon tokens at the end of the chunk so that their attention scopes are the same. It can be observed that such operation results in significant information loss after compression, which justifies the effectiveness of our fine-grained compression mechanism. Secondly, we replace the chunk-wise random compression ratio with the instance-wise one, which randomly selects one compression ratio for each training instance rather than each chunk. We can observe that the chunk-wise setting facilitates better learning of the compression functionality. Lastly, we remove either pre-training or fine-tuning. It can be observe that both stages are useful, and the combination of both leads to the optimal performance. This also implies that the compression quality of Activation Beacon can be further enhanced given more abundant and targeted training.

Table 4: The impact of different technical factors.

| Method | Single-Doc |
|------------------------------|-------------|
| Default | 40.5 |
| w/o Fine-Grained Compression | 35.2 |
| w/o Chunk-Wise Random Ratio | 37.7 |
| w/o Pre-training | 34.9 |
| w/o Fine-tuning | 35.5 |

5 CONCLUSION

This paper introduces Activation Beacon, a plug-in for transformer-based LLMs to enable effective, efficient, and flexible compression of long contexts. Activation Beacon is featured for several critical innovations, including the progressive and fine-grained compression workflow to distill the context into a small set of activations, the compression-based auto-regression to optimize the model with high sample efficiency, and the random sampling of compression ratios to support various downstream scenarios. According to extensive experimental evaluations, Activation Beacon consistently outperforms existing context compression methods across various compression configurations. It even maintains comparable performance to the uncompressed baseline, meanwhile achieving 2x acceleration and 8x KV cache reduction. Moreover, the short-context capabilities of the LLM is well preserved.

REFERENCES

- Ntk-aware scaled rope, 2023. URL https://www.reddit.com/r/LocalLLaMA/comments/141lz7j5/ntkaware_scaled_rope_allows_llama_models_to_have/.
- Joshua Ainslie, James Lee-Thorp, Michiel de Jong, Yury Zemlyanskiy, Federico Lebrón, and Sumit Sanghai. GQA: training generalized multi-query transformer models from multi-head checkpoints. In Houda Bouamor, Juan Pino, and Kalika Bali (eds.), *Proceedings of the 2023 Conference on Empirical Methods in Natural Language Processing, EMNLP 2023, Singapore, December 6-10, 2023*, pp. 4895–4901. Association for Computational Linguistics, 2023. doi: 10.18653/V1/2023.EMNLP-MAIN.298. URL <https://doi.org/10.18653/v1/2023.emnlp-main.298>.
- Yushi Bai, Xin Lv, Jijie Zhang, Hongchang Lyu, Jiankai Tang, Zhidian Huang, Zhengxiao Du, Xiao Liu, Aohan Zeng, Lei Hou, Yuxiao Dong, Jie Tang, and Juanzi Li. Longbench: A bilingual, multitask benchmark for long context understanding. *arXiv preprint arXiv:2308.14508*, 2023.
- Yushi Bai, Jijie Zhang, Xin Lv, Linzhi Zheng, Siqi Zhu, Lei Hou, Yuxiao Dong, Jie Tang, and Juanzi Li. Longwriter: Unleashing 10,000+ word generation from long context llms. *CoRR*, abs/2408.07055, 2024. doi: 10.48550/ARXIV.2408.07055. URL <https://doi.org/10.48550/arXiv.2408.07055>.

- 540 Iz Beltagy, Matthew E. Peters, and Arman Cohan. Longformer: The long-document transformer.
541 *CoRR*, abs/2004.05150, 2020. URL <https://arxiv.org/abs/2004.05150>.
542
- 543 Sumithra Bhakthavatsalam, Daniel Khashabi, Tushar Khot, Bhavana Dalvi Mishra, Kyle Richard-
544 son, Ashish Sabharwal, Carissa Schoenick, Oyvind Tafjord, and Peter Clark. Think you have
545 solved direct-answer question answering? try arc-da, the direct-answer AI2 reasoning challenge.
546 *CoRR*, abs/2102.03315, 2021. URL <https://arxiv.org/abs/2102.03315>.
- 547 William Brandon, Mayank Mishra, Aniruddha Nrusimha, Rameswar Panda, and Jonathan Ragan-
548 Kelley. Reducing transformer key-value cache size with cross-layer attention. *CoRR*,
549 abs/2405.12981, 2024. doi: 10.48550/ARXIV.2405.12981. URL [https://doi.org/10.](https://doi.org/10.48550/arXiv.2405.12981)
550 [48550/arXiv.2405.12981](https://doi.org/10.48550/arXiv.2405.12981).
- 551 Aydar Bulatov, Yuri Kuratov, and Mikhail S. Burtsev. Scaling transformer to 1m tokens and beyond
552 with RMT. *CoRR*, abs/2304.11062, 2023. doi: 10.48550/ARXIV.2304.11062. URL [https://](https://doi.org/10.48550/arXiv.2304.11062)
553 doi.org/10.48550/arXiv.2304.11062.
554
- 555 Shouyuan Chen, Sherman Wong, Liangjian Chen, and Yuandong Tian. Extending context window
556 of large language models via positional interpolation. *arXiv preprint arXiv:2306.15595*, 2023a.
- 557 Yukang Chen, Shengju Qian, Haotian Tang, Xin Lai, Zhijian Liu, Song Han, and Jiaya Jia. Longlora:
558 Efficient fine-tuning of long-context large language models. *arXiv preprint arXiv:2309.12307*,
559 2023b.
- 560 Alexis Chevalier, Alexander Wettig, Anirudh Ajith, and Danqi Chen. Adapting language models to
561 compress contexts. In Houda Bouamor, Juan Pino, and Kalika Bali (eds.), *Proceedings of the 2023*
562 *Conference on Empirical Methods in Natural Language Processing, EMNLP 2023, Singapore,*
563 *December 6-10, 2023*, pp. 3829–3846. Association for Computational Linguistics, 2023. URL
564 <https://aclanthology.org/2023.emnlp-main.232>.
565
- 566 Christopher Clark, Kenton Lee, Ming-Wei Chang, Tom Kwiatkowski, Michael Collins, and Kristina
567 Toutanova. Boolq: Exploring the surprising difficulty of natural yes/no questions. In Jill Burstein,
568 Christy Doran, and Tamar Solorio (eds.), *Proceedings of the 2019 Conference of the North Amer-*
569 *ican Chapter of the Association for Computational Linguistics: Human Language Technologies,*
570 *NAACL-HLT 2019, Minneapolis, MN, USA, June 2-7, 2019, Volume 1 (Long and Short Papers)*,
571 pp. 2924–2936. Association for Computational Linguistics, 2019. doi: 10.18653/v1/N19-1300.
572 URL <https://doi.org/10.18653/v1/n19-1300>.
- 573 Karl Cobbe, Vineet Kosaraju, Mohammad Bavarian, Mark Chen, Heewoo Jun, Lukasz Kaiser,
574 Matthias Plappert, Jerry Tworek, Jacob Hilton, Reiichiro Nakano, Christopher Hesse, and John
575 Schulman. Training verifiers to solve math word problems. *CoRR*, abs/2110.14168, 2021. URL
576 <https://arxiv.org/abs/2110.14168>.
- 577 Together Computer. Redpajama: An open source recipe to reproduce llama training dataset, 2023.
578 URL <https://github.com/togethercomputer/RedPajama-Data>.
579
- 580 Tri Dao. Flashattention-2: Faster attention with better parallelism and work partitioning. *CoRR*,
581 abs/2307.08691, 2023. doi: 10.48550/ARXIV.2307.08691. URL [https://doi.org/10.](https://doi.org/10.48550/arXiv.2307.08691)
582 [48550/arXiv.2307.08691](https://doi.org/10.48550/arXiv.2307.08691).
- 583 DeepSeek-AI. Deepseek-v2: A strong, economical, and efficient mixture-of-experts language
584 model, 2024.
- 585 Yiran Ding, Li Lyna Zhang, Chengruidong Zhang, Yuanyuan Xu, Ning Shang, Jiahang Xu, Fan
586 Yang, and Mao Yang. Longrope: Extending llm context window beyond 2 million tokens, 2024.
587
- 588 Abhimanyu Dubey, Abhinav Jauhri, Abhinav Pandey, Abhishek Kadian, Ahmad Al-Dahle, Aiesha
589 Letman, Akhil Mathur, Alan Schelten, Amy Yang, Angela Fan, Anirudh Goyal, Anthony
590 Hartshorn, Aobo Yang, Archi Mitra, Archie Sravankumar, Artem Korenev, Arthur Hinsvark,
591 Arun Rao, Aston Zhang, Aurelien Rodriguez, Austen Gregerson, Ava Spataru, Baptiste Roziere,
592 Bethany Biron, Binh Tang, Bobbie Chern, Charlotte Caucheteux, Chaya Nayak, Chloe Bi, Chris
593 Marra, Chris McConnell, Christian Keller, Christophe Touret, Chunyang Wu, Corinne Wong,
Cristian Canton Ferrer, Cyrus Nikolaidis, Damien Allonsius, Daniel Song, Danielle Pintz, Danny

594 Livshits, David Esiobu, Dhruv Choudhary, Dhruv Mahajan, Diego Garcia-Olano, Diego Perino,
 595 Dieuwke Hupkes, Egor Lakomkin, Ehab AlBadawy, Elina Lobanova, Emily Dinan, Eric Michael
 596 Smith, Filip Radenovic, Frank Zhang, Gabriel Synnaeve, Gabrielle Lee, Georgia Lewis Ander-
 597 son, Graeme Nail, Gregoire Mialon, Guan Pang, Guillem Cucurell, Hailey Nguyen, Hannah
 598 Korevaar, Hu Xu, Hugo Touvron, Iliyan Zarov, Imanol Arrieta Ibarra, Isabel Kloumann, Ishan
 599 Misra, Ivan Evtimov, Jade Copet, Jaewon Lee, Jan Geffert, Jana Vranes, Jason Park, Jay Ma-
 600 hadeokar, Jeet Shah, Jelmer van der Linde, Jennifer Billock, Jenny Hong, Jenya Lee, Jeremy
 601 Fu, Jianfeng Chi, Jianyu Huang, Jiawen Liu, Jie Wang, Jiecao Yu, Joanna Bitton, Joe Spisak,
 602 Jongsoo Park, Joseph Rocca, Joshua Johnstun, Joshua Saxe, Junteng Jia, Kalyan Vasuden Al-
 603 wala, Kartikeya Upasani, Kate Plawiak, Ke Li, Kenneth Heafield, Kevin Stone, Khalid El-Arini,
 604 Krithika Iyer, Kshitiz Malik, Kuenley Chiu, Kunal Bhalla, Lauren Rantala-Yeary, Laurens van der
 605 Maaten, Lawrence Chen, Liang Tan, Liz Jenkins, Louis Martin, Lovish Madaan, Lubo Malo,
 606 Lukas Blecher, Lukas Landzaat, Luke de Oliveira, Madeline Muzzi, Mahesh Pasupuleti, Man-
 607 nat Singh, Manohar Paluri, Marcin Kardas, Mathew Oldham, Mathieu Rita, Maya Pavlova,
 608 Melanie Kambadur, Mike Lewis, Min Si, Mitesh Kumar Singh, Mona Hassan, Naman Goyal,
 609 Narjes Torabi, Nikolay Bashlykov, Nikolay Bogoychev, Niladri Chatterji, Olivier Duchenne, Onur
 610 Çelebi, Patrick Alrassy, Pengchuan Zhang, Pengwei Li, Petar Vasic, Peter Weng, Prajjwal Bhar-
 611 gava, Pratik Dubal, Praveen Krishnan, Punit Singh Koura, Puxin Xu, Qing He, Qingxiao Dong,
 612 Ragavan Srinivasan, Raj Ganapathy, Ramon Calderer, Ricardo Silveira Cabral, Robert Stojnic,
 613 Roberta Raileanu, Rohit Girdhar, Rohit Patel, Romain Sauvestre, Ronnie Polidoro, Roshan Sum-
 614 baly, Ross Taylor, Ruan Silva, Rui Hou, Rui Wang, Saghar Hosseini, Sahana Chennabasappa,
 615 Sanjay Singh, Sean Bell, Seohyun Sonia Kim, Sergey Edunov, Shaoliang Nie, Sharan Narang,
 616 Sharath Raparthy, Sheng Shen, Shengye Wan, Shruti Bhosale, Shun Zhang, Simon Vandenhende,
 617 Soumya Batra, Spencer Whitman, Sten Sootla, Stephane Collot, Suchin Gururangan, Sydney
 618 Borodinsky, Tamar Herman, Tara Fowler, Tarek Sheasha, Thomas Georgiou, Thomas Scialom,
 619 Tobias Speckbacher, Todor Mihaylov, Tong Xiao, Ujjwal Karn, Vedanuj Goswami, Vibhor Gupta,
 620 Vignesh Ramanathan, Viktor Kerkez, Vincent Gonguet, Virginie Do, Vish Vogeti, Vladan Petro-
 621 vic, Weiwei Chu, Wenhan Xiong, Wenyin Fu, Whitney Meers, Xavier Martinet, Xiaodong Wang,
 622 Xiaoqing Ellen Tan, Xinfeng Xie, Xuchao Jia, Xuwei Wang, Yaelle Goldschlag, Yashesh Gaur,
 623 Yasmine Babaei, Yi Wen, Yiwen Song, Yuchen Zhang, Yue Li, Yuning Mao, Zacharie Delpierre
 624 Coudert, Zheng Yan, Zhengxing Chen, Zoe Papakipos, Aaditya Singh, Aaron Grattafiori, Abha
 625 Jain, Adam Kelsey, Adam Shajnfeld, Adithya Gangidi, Adolfo Victoria, Ahuva Goldstand, Ajay
 626 Menon, Ajay Sharma, Alex Boesenberg, Alex Vaughan, Alexei Baevski, Allie Feinstein, Amanda
 627 Kallet, Amit Sangani, Anam Yunus, Andrei Lupu, Andres Alvarado, Andrew Caples, Andrew
 628 Gu, Andrew Ho, Andrew Poulton, Andrew Ryan, Ankit Ramchandani, Annie Franco, Aparajita
 629 Saraf, Arkabandhu Chowdhury, Ashley Gabriel, Ashwin Bharambe, Assaf Eisenman, Azadeh
 630 Yazdan, Beau James, Ben Maurer, Benjamin Leonhardi, Bernie Huang, Beth Loyd, Beto De
 631 Paola, Bhargavi Paranjape, Bing Liu, Bo Wu, Boyu Ni, Braden Hancock, Bram Wasti, Bran-
 632 don Spence, Brani Stojkovic, Brian Gamido, Britt Montalvo, Carl Parker, Carly Burton, Catalina
 633 Mejia, Changhan Wang, Changkyu Kim, Chao Zhou, Chester Hu, Ching-Hsiang Chu, Chris Cai,
 634 Chris Tindal, Christoph Feichtenhofer, Damon Civin, Dana Beaty, Daniel Kreymer, Daniel Li,
 635 Danny Wyatt, David Adkins, David Xu, Davide Testuggine, Delia David, Devi Parikh, Diana
 636 Liskovich, Didem Foss, Dingkang Wang, Duc Le, Dustin Holland, Edward Dowling, Eissa Jamil,
 637 Elaine Montgomery, Eleonora Presani, Emily Hahn, Emily Wood, Erik Brinkman, Esteban Ar-
 638 caute, Evan Dunbar, Evan Smothers, Fei Sun, Felix Kreuk, Feng Tian, Firat Ozgenel, Francesco
 639 Caggioni, Francisco Guzmán, Frank Kanayet, Frank Seide, Gabriela Medina Florez, Gabriella
 640 Schwarz, Gada Badeer, Georgia Swee, Gil Halpern, Govind Thattai, Grant Herman, Grigory
 641 Sizov, Guangyi, Zhang, Guna Lakshminarayanan, Hamid Shojanazeri, Han Zou, Hannah Wang,
 642 Hanwen Zha, Haroun Habeeb, Harrison Rudolph, Helen Suk, Henry Aspegren, Hunter Gold-
 643 man, Ibrahim Damlaj, Igor Molybog, Igor Tufanov, Irina-Elena Veliche, Itai Gat, Jake Weissman,
 644 James Geboski, James Kohli, Japhet Asher, Jean-Baptiste Gaya, Jeff Marcus, Jeff Tang, Jennifer
 645 Chan, Jenny Zhen, Jeremy Reizenstein, Jeremy Teboul, Jessica Zhong, Jian Jin, Jingyi Yang, Joe
 646 Cummings, Jon Carvill, Jon Shepard, Jonathan McPhee, Jonathan Torres, Josh Ginsburg, Junjie
 647 Wang, Kai Wu, Kam Hou U, Karan Saxena, Karthik Prasad, Kartikay Khandelwal, Katayoun
 Zand, Kathy Matosich, Kaushik Veeraraghavan, Kelly Michelena, Keqian Li, Kun Huang, Kunal
 Chawla, Kushal Lakhotia, Kyle Huang, Lailin Chen, Lakshya Garg, Lavender A, Leandro Silva,
 Lee Bell, Lei Zhang, Liangpeng Guo, Licheng Yu, Liron Moshkovich, Luca Wehrstedt, Madian
 Khabsa, Manav Avalani, Manish Bhatt, Maria Tsimpoukelli, Martynas Mankus, Matan Hasson,
 Matthew Lennie, Matthias Reso, Maxim Groshev, Maxim Naumov, Maya Lathi, Meghan Ke-

- 648 neally, Michael L. Seltzer, Michal Valko, Michelle Restrepo, Mihir Patel, Mik Vyatskov, Mikayel
649 Samvelyan, Mike Clark, Mike Macey, Mike Wang, Miquel Jubert Hermoso, Mo Metanat, Mo-
650 hammad Rastegari, Munish Bansal, Nandhini Santhanam, Natascha Parks, Natasha White, Navy-
651 ata Bawa, Nayan Singhal, Nick Egebo, Nicolas Usunier, Nikolay Pavlovich Laptev, Ning Dong,
652 Ning Zhang, Norman Cheng, Oleg Chernoguz, Olivia Hart, Omkar Salpekar, Ozlem Kalinli,
653 Parkin Kent, Parth Parekh, Paul Saab, Pavan Balaji, Pedro Rittner, Philip Bontrager, Pierre Roux,
654 Piotr Dollar, Polina Zvyagina, Prashant Ratanchandani, Pritish Yuvraj, Qian Liang, Rachad Alao,
655 Rachel Rodriguez, Rafi Ayub, Raghotham Murthy, Raghu Nayani, Rahul Mitra, Raymond Li,
656 Rebekkah Hogan, Robin Battey, Rocky Wang, Rohan Maheswari, Russ Howes, Ruty Rinott,
657 Sai Jayesh Bondu, Samyak Datta, Sara Chugh, Sara Hunt, Sargun Dhillon, Sasha Sidorov, Sa-
658 tadru Pan, Saurabh Verma, Seiji Yamamoto, Sharadh Ramaswamy, Shaun Lindsay, Shaun Lind-
659 say, Sheng Feng, Shenghao Lin, Shengxin Cindy Zha, Shiva Shankar, Shuqiang Zhang, Shuqiang
660 Zhang, Sinong Wang, Sneha Agarwal, Soji Sajuyigbe, Soumith Chintala, Stephanie Max, Stephen
661 Chen, Steve Kehoe, Steve Satterfield, Sudarshan Govindaprasad, Sumit Gupta, Sungmin Cho,
662 Sunny Virk, Suraj Subramanian, Sy Choudhury, Sydney Goldman, Tal Remez, Tamar Glaser,
663 Tamara Best, Thilo Kohler, Thomas Robinson, Tianhe Li, Tianjun Zhang, Tim Matthews, Tim-
664 othy Chou, Tzook Shaked, Varun Vontimitta, Victoria Ajayi, Victoria Montanez, Vijai Mohan,
665 Vinay Satish Kumar, Vishal Mangla, Vitor Albiero, Vlad Ionescu, Vlad Poenaru, Vlad Tiberiu
666 Mihailescu, Vladimir Ivanov, Wei Li, Wenchen Wang, Wenwen Jiang, Wes Bouaziz, Will Con-
667 stable, Xiaocheng Tang, Xiaofang Wang, Xiaoqian Wu, Xiaolan Wang, Xide Xia, Xilun Wu,
668 Xinbo Gao, Yanjun Chen, Ye Hu, Ye Jia, Ye Qi, Yenda Li, Yilin Zhang, Ying Zhang, Yossi Adi,
669 Youngjin Nam, Yu, Wang, Yuchen Hao, Yundi Qian, Yuzi He, Zach Rait, Zachary DeVito, Zef
670 Rosnbrick, Zhaoduo Wen, Zhenyu Yang, and Zhiwei Zhao. The llama 3 herd of models, 2024.
URL <https://arxiv.org/abs/2407.21783>.
- 671 Leo Gao, Stella Biderman, Sid Black, Laurence Golding, Travis Hoppe, Charles Foster, Jason
672 Phang, Horace He, Anish Thite, Noa Nabeshima, Shawn Presser, and Connor Leahy. The pile:
673 An 800gb dataset of diverse text for language modeling, 2020.
- 674 Tao Ge, Jing Hu, Lei Wang, Xun Wang, Si-Qing Chen, and Furu Wei. In-context autoencoder for
675 context compression in a large language model, 2024.
- 676
- 677 gkamradt, 2023. URL [https://github.com/gkamradt/LLMTest_](https://github.com/gkamradt/LLMTest_NeedleInAHaystack)
678 [NeedleInAHaystack](https://github.com/gkamradt/LLMTest_NeedleInAHaystack).
- 679
- 680 Chi Han, Qifan Wang, Wenhan Xiong, Yu Chen, Heng Ji, and Sinong Wang. Lm-infinite: Simple
681 on-the-fly length generalization for large language models. *CoRR*, abs/2308.16137, 2023. doi: 10.
682 48550/ARXIV.2308.16137. URL <https://doi.org/10.48550/arXiv.2308.16137>.
- 683 Dan Hendrycks, Collin Burns, Steven Basart, Andy Zou, Mantas Mazeika, Dawn Song, and Jacob
684 Steinhardt. Measuring massive multitask language understanding. In *9th International Confer-*
685 *ence on Learning Representations, ICLR 2021, Virtual Event, Austria, May 3-7, 2021*. OpenRe-
686 view.net, 2021. URL <https://openreview.net/forum?id=d7KBjmI3GmQ>.
- 687
- 688 Cheng-Ping Hsieh, Simeng Sun, Samuel Kriman, Shantanu Acharya, Dima Rekeshe, Fei Jia, Yang
689 Zhang, and Boris Ginsburg. RULER: what’s the real context size of your long-context language
690 models? *CoRR*, abs/2404.06654, 2024. doi: 10.48550/ARXIV.2404.06654. URL <https://doi.org/10.48550/arXiv.2404.06654>.
- 691
- 692 Huiqiang Jiang, Qianhui Wu, Chin-Yew Lin, Yuqing Yang, and Lili Qiu. Llmlingua: Compressing
693 prompts for accelerated inference of large language models. *arXiv preprint arXiv:2310.05736*,
694 2023a.
- 695
- 696 Huiqiang Jiang, Qianhui Wu, Xufang Luo, Dongsheng Li, Chin-Yew Lin, Yuqing Yang, and Lili
697 Qiu. Longllmlingua: Accelerating and enhancing llms in long context scenarios via prompt com-
698 pression, 2023b.
- 699
- 700 Huiqiang Jiang, Yucheng Li, Chengruidong Zhang, Qianhui Wu, Xufang Luo, Surin Ahn, Zhenhua
701 Han, Amir H. Abdi, Dongsheng Li, Chin-Yew Lin, Yuqing Yang, and Lili Qiu. Minference
1.0: Accelerating pre-filling for long-context llms via dynamic sparse attention, 2024a. URL
<https://arxiv.org/abs/2407.02490>.

- 702 Ziyan Jiang, Xueguang Ma, and Wenhua Chen. Longrag: Enhancing retrieval-augmented generation
703 with long-context llms. *CoRR*, abs/2406.15319, 2024b. doi: 10.48550/ARXIV.2406.15319. URL
704 <https://doi.org/10.48550/arXiv.2406.15319>.
- 705
706 Jang-Hyun Kim, Junyoung Yeom, Sangdoon Yun, and Hyun Oh Song. Compressed context memory
707 for online language model interaction, 2024.
- 708 Wojciech Kryściński, Nazneen Rajani, Divyansh Agarwal, Caiming Xiong, and Dragomir Radev.
709 Booksum: A collection of datasets for long-form narrative summarization, 2022.
- 710
711 Mo Li, Songyang Zhang, Yunxin Liu, and Kai Chen. Needlebench: Can llms do retrieval and
712 reasoning in 1 million context window?, 2024a. URL <https://arxiv.org/abs/2407.11963>.
- 713
714 Yuhong Li, Yingbing Huang, Bowen Yang, Bharat Venkitesh, Acyr Locatelli, Hanchen Ye, Tianle
715 Cai, Patrick Lewis, and Deming Chen. Snapkv: Llm knows what you are looking for before
716 generation, 2024b. URL <https://arxiv.org/abs/2404.14469>.
- 717
718 Yuhan Liu, Hanchen Li, Kuntai Du, Jiayi Yao, Yihua Cheng, Yuyang Huang, Shan Lu,
719 Michael Maire, Henry Hoffmann, Ari Holtzman, Ganesh Ananthanarayanan, and Junchen Jiang.
720 Cachegen: Fast context loading for language model applications. *CoRR*, abs/2310.07240, 2023.
721 doi: 10.48550/ARXIV.2310.07240. URL <https://doi.org/10.48550/arXiv.2310.07240>.
- 722
723 Jesse Mu, Xiang Lisa Li, and Noah D. Goodman. Learning to compress prompts with gist tokens.
724 *CoRR*, abs/2304.08467, 2023. doi: 10.48550/ARXIV.2304.08467. URL <https://doi.org/10.48550/arXiv.2304.08467>.
- 725
726 OpenAI, Josh Achiam, Steven Adler, Sandhini Agarwal, Lama Ahmad, Ilge Akkaya, Floren-
727 cia Leoni Aleman, Diogo Almeida, Janko Altenschmidt, Sam Altman, Shyamal Anadkat, Red
728 Avila, Igor Babuschkin, Suchir Balaji, Valerie Balcom, Paul Baltescu, Haiming Bao, Moham-
729 mad Bavarian, Jeff Belgum, Irwan Bello, Jake Berdine, Gabriel Bernadett-Shapiro, Christopher
730 Berner, Lenny Bogdonoff, Oleg Boiko, Madelaine Boyd, Anna-Luisa Brakman, Greg Brock-
731 man, Tim Brooks, Miles Brundage, Kevin Button, Trevor Cai, Rosie Campbell, Andrew Cann,
732 Brittany Carey, Chelsea Carlson, Rory Carmichael, Brooke Chan, Che Chang, Fotis Chantzis,
733 Derek Chen, Sully Chen, Ruby Chen, Jason Chen, Mark Chen, Ben Chess, Chester Cho, Casey
734 Chu, Hyung Won Chung, Dave Cummings, Jeremiah Currier, Yunxing Dai, Cory Decareaux,
735 Thomas Degry, Noah Deutsch, Damien Deville, Arka Dhar, David Dohan, Steve Dowling, Sheila
736 Dunning, Adrien Ecoffet, Atty Eleti, Tyna Eloundou, David Farhi, Liam Fedus, Niko Felix,
737 Simón Posada Fishman, Juston Forte, Isabella Fulford, Leo Gao, Elie Georges, Christian Gib-
738 son, Vik Goel, Tarun Gogineni, Gabriel Goh, Rapha Gontijo-Lopes, Jonathan Gordon, Morgan
739 Grafstein, Scott Gray, Ryan Greene, Joshua Gross, Shixiang Shane Gu, Yufei Guo, Chris Hal-
740 lacy, Jesse Han, Jeff Harris, Yuchen He, Mike Heaton, Johannes Heidecke, Chris Hesse, Alan
741 Hickey, Wade Hickey, Peter Hoeschele, Brandon Houghton, Kenny Hsu, Shengli Hu, Xin Hu,
742 Joost Huizinga, Shantanu Jain, Shawn Jain, Joanne Jang, Angela Jiang, Roger Jiang, Haozhun
743 Jin, Denny Jin, Shino Jomoto, Billie Jonn, Heewoo Jun, Tomer Kaftan, Łukasz Kaiser, Ali Kam-
744 mali, Ingmar Kanitscheider, Nitish Shirish Keskar, Tabarak Khan, Logan Kilpatrick, Jong Wook
745 Kim, Christina Kim, Yongjik Kim, Jan Hendrik Kirchner, Jamie Kiros, Matt Knight, Daniel
746 Kokotajlo, Łukasz Kondraciuk, Andrew Kondrich, Aris Konstantinidis, Kyle Kosic, Gretchen
747 Krueger, Vishal Kuo, Michael Lampe, Ikai Lan, Teddy Lee, Jan Leike, Jade Leung, Daniel
748 Levy, Chak Ming Li, Rachel Lim, Molly Lin, Stephanie Lin, Mateusz Litwin, Theresa Lopez,
749 Ryan Lowe, Patricia Lue, Anna Makanju, Kim Malfacini, Sam Manning, Todor Markov, Yaniv
750 Markovski, Bianca Martin, Katie Mayer, Andrew Mayne, Bob McGrew, Scott Mayer McKinney,
751 Christine McLeavey, Paul McMillan, Jake McNeil, David Medina, Aalok Mehta, Jacob Menick,
752 Luke Metz, Andrey Mishchenko, Pamela Mishkin, Vinnie Monaco, Evan Morikawa, Daniel
753 Mossing, Tong Mu, Mira Murati, Oleg Murk, David Mély, Ashvin Nair, Reiichiro Nakano, Ra-
754 jeev Nayak, Arvind Neelakantan, Richard Ngo, Hyeonwoo Noh, Long Ouyang, Cullen O’Keefe,
755 Jakub Pachocki, Alex Paino, Joe Palermo, Ashley Pantuliano, Giambattista Parascandolo, Joel
Parish, Emy Parparita, Alex Passos, Mikhail Pavlov, Andrew Peng, Adam Perelman, Filipe
de Avila Belbute Peres, Michael Petrov, Henrique Ponde de Oliveira Pinto, Michael, Pokorny,
Michelle Pokrass, Vitchyr H. Pong, Tolly Powell, Alethea Power, Boris Power, Elizabeth Proehl,

- 756 Raul Puri, Alec Radford, Jack Rae, Aditya Ramesh, Cameron Raymond, Francis Real, Kendra
757 Rimbach, Carl Ross, Bob Rotsted, Henri Roussez, Nick Ryder, Mario Saltarelli, Ted Sanders,
758 Shibani Santurkar, Girish Sastry, Heather Schmidt, David Schnurr, John Schulman, Daniel Sel-
759 sam, Kyla Sheppard, Toki Sherbakov, Jessica Shieh, Sarah Shoker, Pranav Shyam, Szymon Sidor,
760 Eric Sigler, Maddie Simens, Jordan Sitkin, Katarina Slama, Ian Sohl, Benjamin Sokolowsky,
761 Yang Song, Natalie Staudacher, Felipe Petroski Such, Natalie Summers, Ilya Sutskever, Jie Tang,
762 Nikolas Tezak, Madeleine B. Thompson, Phil Tillet, Amin Tootoonchian, Elizabeth Tseng, Pre-
763 ston Tuggle, Nick Turley, Jerry Tworek, Juan Felipe Cerón Uribe, Andrea Vallone, Arun Vi-
764 jayvergiya, Chelsea Voss, Carroll Wainwright, Justin Jay Wang, Alvin Wang, Ben Wang, Jonathan
765 Ward, Jason Wei, CJ Weinmann, Akila Welihinda, Peter Welinder, Jiayi Weng, Lilian Weng,
766 Matt Wiethoff, Dave Willner, Clemens Winter, Samuel Wolrich, Hannah Wong, Lauren Work-
767 man, Sherwin Wu, Jeff Wu, Michael Wu, Kai Xiao, Tao Xu, Sarah Yoo, Kevin Yu, Qiming
768 Yuan, Wojciech Zaremba, Rowan Zellers, Chong Zhang, Marvin Zhang, Shengjia Zhao, Tianhao
769 Zheng, Juntang Zhuang, William Zhuk, and Barret Zoph. Gpt-4 technical report, 2024. URL
770 <https://arxiv.org/abs/2303.08774>.
- 771 Bowen Peng, Jeffrey Quesnelle, Honglu Fan, and Enrico Shippole. Yarn: Efficient context window
772 extension of large language models. *arXiv preprint arXiv:2309.00071*, 2023.
- 773 Jianlin Su, Yu Lu, Shengfeng Pan, Bo Wen, and Yunfeng Liu. Roformer: Enhanced transformer
774 with rotary position embedding. *CoRR*, abs/2104.09864, 2021. URL <https://arxiv.org/abs/2104.09864>.
- 775
776
- 777 Sijun Tan, Xiuyu Li, Shishir G. Patil, Ziyang Wu, Tianjun Zhang, Kurt Keutzer, Joseph Gon-
778 zalez, and Raluca A. Popa. Lloc: Learning long contexts offline. In Yaser Al-Onaizan,
779 Mohit Bansal, and Yun-Nung Chen (eds.), *Proceedings of the 2024 Conference on Empiri-
780 cal Methods in Natural Language Processing, EMNLP 2024, Miami, FL, USA, November 12-
781 16, 2024*, pp. 17605–17621. Association for Computational Linguistics, 2024. URL <https://aclanthology.org/2024.emnlp-main.975>.
- 782
- 783 Hugo Touvron, Louis Martin, Kevin Stone, Peter Albert, Amjad Almahairi, Yasmine Babaei, Niko-
784 lay Bashlykov, Soumya Batra, Prajjwal Bhargava, Shruti Bhosale, Dan Bikel, Lukas Blecher,
785 Cristian Canton Ferrer, Moya Chen, Guillem Cucurull, David Esiobu, Jude Fernandes, Jeremy
786 Fu, Wenyin Fu, Brian Fuller, Cynthia Gao, Vedanuj Goswami, Naman Goyal, Anthony Hartshorn,
787 Saghar Hosseini, Rui Hou, Hakan Inan, Marcin Kardas, Viktor Kerkez, Madian Khabsa, Isabel
788 Kloumann, Artem Korenev, Punit Singh Koura, Marie-Anne Lachaux, Thibaut Lavril, Jenya Lee,
789 Diana Liskovich, Yinghai Lu, Yuning Mao, Xavier Martinet, Todor Mihaylov, Pushkar Mishra,
790 Igor Molybog, Yixin Nie, Andrew Poulton, Jeremy Reizenstein, Rashi Rungta, Kalyan Saladi,
791 Alan Schelten, Ruan Silva, Eric Michael Smith, Ranjan Subramanian, Xiaoqing Ellen Tan, Binh
792 Tang, Ross Taylor, Adina Williams, Jian Xiang Kuan, Puxin Xu, Zheng Yan, Iliyan Zarov, Yuchen
793 Zhang, Angela Fan, Melanie Kambadur, Sharan Narang, Aurelien Rodriguez, Robert Stojnic,
794 Sergey Edunov, and Thomas Scialom. Llama 2: Open foundation and fine-tuned chat models,
795 2023.
- 796 Thomas Wolf, Lysandre Debut, Victor Sanh, Julien Chaumond, Clement Delangue, Anthony Moi,
797 Pierric Cistac, Tim Rault, Rémi Louf, Morgan Funtowicz, Joe Davison, Sam Shleifer, Patrick
798 von Platen, Clara Ma, Yacine Jernite, Julien Plu, Canwen Xu, Teven Le Scao, Sylvain Gugger,
799 Mariama Drame, Quentin Lhoest, and Alexander M. Rush. Huggingface’s transformers: State-of-
800 the-art natural language processing, 2020. URL <https://arxiv.org/abs/1910.03771>.
- 801 Chaojun Xiao, Pengle Zhang, Xu Han, Guangxuan Xiao, Yankai Lin, Zhengyan Zhang, Zhiyuan
802 Liu, and Maosong Sun. Inflm: Training-free long-context extrapolation for llms with an efficient
803 context memory, 2024. URL <https://arxiv.org/abs/2402.04617>.
- 804 Guangxuan Xiao, Yuandong Tian, Beidi Chen, Song Han, and Mike Lewis. Efficient streaming
805 language models with attention sinks. *arXiv preprint arXiv:2309.17453*, 2023.
- 806
- 807 An Yang, Baosong Yang, Binyuan Hui, Bo Zheng, Bowen Yu, Chang Zhou, Chengpeng Li,
808 Chengyuan Li, Dayiheng Liu, Fei Huang, Guanting Dong, Haoran Wei, Huan Lin, Jialong Tang,
809 Jialin Wang, Jian Yang, Jianhong Tu, Jianwei Zhang, Jianxin Ma, Jianxin Yang, Jin Xu, Jingren
Zhou, Jinze Bai, Jinzheng He, Junyang Lin, Kai Dang, Keming Lu, Keqin Chen, Kexin Yang,

- 810 Mei Li, Mingfeng Xue, Na Ni, Pei Zhang, Peng Wang, Ru Peng, Rui Men, Ruize Gao, Runji Lin,
811 Shijie Wang, Shuai Bai, Sinan Tan, Tianhang Zhu, Tianhao Li, Tianyu Liu, Wenbin Ge, Xiaodong
812 Deng, Xiaohuan Zhou, Xingzhang Ren, Xinyu Zhang, Xipin Wei, Xuancheng Ren, Xuejing Liu,
813 Yang Fan, Yang Yao, Yichang Zhang, Yu Wan, Yunfei Chu, Yuqiong Liu, Zeyu Cui, Zhenru
814 Zhang, Zhifang Guo, and Zhihao Fan. Qwen2 technical report. *CoRR*, abs/2407.10671, 2024.
815 doi: 10.48550/ARXIV.2407.10671. URL [https://doi.org/10.48550/arXiv.2407.](https://doi.org/10.48550/arXiv.2407.10671)
816 10671.
- 817 Howard Yen, Tianyu Gao, and Danqi Chen. Long-context language modeling with parallel context
818 encoding. In Lun-Wei Ku, Andre Martins, and Vivek Srikumar (eds.), *Proceedings of the 62nd*
819 *Annual Meeting of the Association for Computational Linguistics (Volume 1: Long Papers), ACL*
820 *2024, Bangkok, Thailand, August 11-16, 2024*, pp. 2588–2610. Association for Computational
821 Linguistics, 2024. doi: 10.18653/V1/2024.ACL-LONG.142. URL [https://doi.org/10.](https://doi.org/10.18653/v1/2024.acl-long.142)
822 18653/v1/2024.acl-long.142.
- 823 Manzil Zaheer, Guru Guruganesh, Kumar Avinava Dubey, Joshua Ainslie, Chris Alberti, Santiago
824 Ontanon, Philip Pham, Anirudh Ravula, Qifan Wang, Li Yang, et al. Big bird: Transformers for
825 longer sequences. *Advances in neural information processing systems*, 33:17283–17297, 2020.
826
- 827 Zeyu Zhang, Xiaohe Bo, Chen Ma, Rui Li, Xu Chen, Quanyu Dai, Jieming Zhu, Zhenhua Dong,
828 and Ji-Rong Wen. A survey on the memory mechanism of large language model based agents.
829 *CoRR*, abs/2404.13501, 2024. doi: 10.48550/ARXIV.2404.13501. URL [https://doi.org/](https://doi.org/10.48550/arXiv.2404.13501)
830 10.48550/arXiv.2404.13501.
- 831 Zhenyu Zhang, Ying Sheng, Tianyi Zhou, Tianlong Chen, Lianmin Zheng, Ruisi Cai, Zhao Song,
832 Yuandong Tian, Christopher Ré, Clark W. Barrett, Zhangyang Wang, and Beidi Chen. H2O:
833 heavy-hitter oracle for efficient generative inference of large language models. In Alice Oh,
834 Tristan Naumann, Amir Globerson, Kate Saenko, Moritz Hardt, and Sergey Levine (eds.),
835 *Advances in Neural Information Processing Systems 36: Annual Conference on Neural In-*
836 *formation Processing Systems 2023, NeurIPS 2023, New Orleans, LA, USA, December 10 -*
837 *16, 2023*, 2023. URL [http://papers.nips.cc/paper_files/paper/2023/hash/](http://papers.nips.cc/paper_files/paper/2023/hash/6ceefa7b15572587b78ecfceb2827f8-Abstract-Conference.html)
838 6ceefa7b15572587b78ecfceb2827f8-Abstract-Conference.html.
- 839 Qianchao Zhu, Jiangfei Duan, Chang Chen, Siran Liu, Xiuhong Li, Guanyu Feng, Xin Lv, Huanqi
840 Cao, Xiao Chuanfu, Xingcheng Zhang, Dahua Lin, and Chao Yang. Sampleattention: Near-
841 lossless acceleration of long context LLM inference with adaptive structured sparse attention.
842 *CoRR*, abs/2406.15486, 2024. doi: 10.48550/ARXIV.2406.15486. URL [https://doi.org/](https://doi.org/10.48550/arXiv.2406.15486)
843 10.48550/arXiv.2406.15486.
- 844 Zirui Liu, Jiayi Yuan, Hongye Jin, Shaochen Zhong, Zhaozhuo Xu, Vladimir Braverman, Beidi
845 Chen, and Xia Hu. Kivi : Plug-and-play 2bit kv cache quantization with streaming asymmetric
846 quantization. 2023. doi: 10.13140/RG.2.2.28167.37282. URL [https://rgdoi.net/10.](https://rgdoi.net/10.13140/RG.2.2.28167.37282)
847 13140/RG.2.2.28167.37282.
848
849
850
851
852
853
854
855
856
857
858
859
860
861
862
863

A TRAINING DATA

In the pre-training phase, we use 1B tokens from RedPajama. We add an eos token to the end of each document. The documents longer than 20480 or shorter than 2400 are removed.

Prompt A.1

```
{Segment 1}
...
{Segment N}

Question: {Question 1 for Segment 1}
Answer: {Answer 1 for Segment 1}
...
Question: {Question 4 for Segment N}
Answer: {Answer 4 for Segment N}
```

In the fine-tuning phase, we use three datasets. 1) LongAlpaca (Chen et al., 2023b), which contains long-context QA and summarization data; 2) BookSum (Kryściński et al., 2022), which contains chapter-level summarization of books. 3) Synthesized QA dataset. This dataset contains 16K long-context question answering instances (13K for books and 3K for papers). Specifically, we split a given long context (a paper or a book) into short segments (a chunk with less than 4096 tokens) using the SemanticTextSplitter³. For each segment, we prompt GPT-3.5-turbo to generate 4 question-answer pairs based on the segment. We then group continuous segments using Template A.1, where we can control the resulted context length by concatenating different number of segments. The books are randomly sampled from Books3 corpus, and the papers are sampled from Arxiv, both coming from the Pile (Gao et al., 2020). All the above fine-tuning data are formatted in the manner of multi-turn conversations and limit the context length up to 20480. To mitigate forgetting, we also include 5000 samples from the pre-training data.

B FLOPS CALCULATION

Denote the input sequence length as s , the cached sequence length as s^{pst} , query head number as h^q , key/value head number as h^k , the hidden size D , head dimension as d , intermediate size I , and vocabulary size V .

$$\begin{aligned}
 F^{Att} &= F^{qkv} + F^{qk} + F^{softmax} + F^{av} + F^{out} \\
 F^{qkv} &= 2 \times s \times D \times d \times h^q + 2 \times 2 \times s \times D \times d \times h^k \\
 F^{qk} &= 2 \times h^q \times s \times (s + s^{pst}) \times d \\
 F^{softmax} &= h^q \times (s + s^{pst}) \times (s + s^{pst}) \\
 F^{av} &= 2 \times h^q \times s \times (s + s^{pst}) \times d \\
 F^{out} &= 2 \times s \times d \times h^q \times D
 \end{aligned} \tag{12}$$

$$\begin{aligned}
 F^{Oth} &= F^{up} + F^{gate} + F^{down} + F^{lm} \\
 F^{up} &= 2 \times s \times D \times 2 \times I \\
 F^{gate} &= s \times I \\
 F^{down} &= 2 \times s \times D \times I \\
 F^{lm} &= 2 \times s \times D \times V
 \end{aligned} \tag{13}$$

³<https://github.com/benbrandt/text-splitter>

Table 5: Comparison of the breakdown latency of prefilling and decoding, as well as peak GPU memory between the full-attention baseline and Activation Beacon. Activation Beacon uses x8 compression uniformly.

| Model | Input Length | Method | Prefilling | Decoding | Total | GPU Memory |
|--------------|--------------|--------|------------|----------|-------|------------|
| Qwen-2.5-7B | 32K | Full | 0.522 | 0.709 | 1.231 | 27.0 |
| | | Ours | 0.514 | 0.506 | 1.020 | 18.1 |
| | 128K | Full | 3.312 | 2.081 | 5.393 | 64.3 |
| | | Ours | 2.038 | 0.550 | 2.588 | 24.6 |
| Qwen-2.5-14B | 32K | Full | 0.952 | 1.862 | 2.814 | 45.7 |
| | | Ours | 0.996 | 0.857 | 1.853 | 36.0 |
| | 128K | Full | – | – | – | OOM |
| | | Ours | 4.340 | 1.117 | 5.457 | 40.3 |

Table 6: Comparison of the training time and the peak GPU memory usage during training between Full-FT and Activation Beacon.

| Model | Method | DeepSpeed Stage | Training Time | GPU Memory |
|--------------|---------|------------------------|---------------|------------|
| Qwen-2.5-7B | Full-FT | Zero-2 | 6.32 | 51.2 |
| | Ours | Zero-2 | 6.58 | 38.5 |
| Qwen-2.5-14B | Full-FT | Zero-3 (OOM w/ Zero-2) | 18.67 | 79.4 |
| | Ours | Zero-2 | 12.34 | 75.6 |

C ADDITIONAL EFFICIENCY ANALYSIS

We further evaluate the efficiency of Activation Beacon by decomposing the latency of pre-filling and decoding. Specifically, we set the context length to 32K and 128K and enforce the model to generate precisely 128 tokens. We use a uniform x8 compression ratio. The peak GPU memory during the entire generation process is also reported.

According to Table 5, our method accelerates both pre-filling and decoding, and the acceleration extent amplifies as the context gets longer. Meanwhile, our method is better at speeding up decoding because it directly conditions on the beacon tokens’ activations, which are 8x shorter than the raw activations used by the baseline. Moreover, Activation Beacon significantly reduces the peak GPU memory usage, enabling efficient processing of long context on customer GPUs.

Lastly, we also compare the training efficiency of Activation Beacon against the standard fine-tuning. The results are shown in Table 6. The experiment result indicates that Activation Beacon achieves comparable training speed as the Full-FT baseline while significantly reducing the memory cost.

D RULER EVALUATION

In addition to LongBench and NIAH, we evaluate the performance of Activation Beacon on RULER (Hsieh et al., 2024), a challenging long-context benchmark that consists of 13 synthetic tasks. Concretely, there are 6 tasks extending the regular NIAH to multi-key, multi-value, and multi-query variants; 1 task (Variable Tracking) aiming at examining the multi-hop reasoning capability by tracking variable assignments; 2 tasks (Common/Frequent Words Extraction) targeting on the aggregation capability by counting the word occurrences; and 2 tasks performing question answering while inserting noisy context to the ground-truth passages. Our evaluation is based on 128K context length and x4 compress ratio for Activation Beacon. The results are shown in Table 7.

It can be observed that our initial Activation Beacon model (denoted as “Ours”) maintains a competitive performance on QA tasks, while lagging far behind the full-attention baseline on reasoning/aggregation tasks (VT and CWE). A similar drop can also be observed on Full-FT, too. One likely reason for this disadvantage is that our current fine-tuning recipe only uses one-hop QA data (as stated in Appedix A), which does not teach the model to perform complex reasoning or count-

Table 7: Evaluation on RULER (Hsieh et al., 2024). Initially, Activation Beacon lags behind full-attention models on reasoning/aggregation tasks, yet the gap can be easily compensated by additional fine-tuning with synthetic 200 samples.

| Model | Method | NIAH AVG | VT | CWE | FWE | QA AVG |
|-------------|---------------------|----------|-------|-------|-------|--------|
| Qwen-2.5-7B | Full | 79.06 | 88.00 | 41.04 | 66.67 | 40.25 |
| | Full-FT | 80.13 | 71.95 | 32.28 | 64.76 | 52.38 |
| | Ours | 78.43 | 25.30 | 10.12 | 60.00 | 52.15 |
| | Ours + Synthetic FT | 80.91 | 85.30 | 59.30 | 72.18 | 51.27 |

Table 8: Evaluation of 7B and 14B models on LongBench (Bai et al., 2023). Activation Beacon always maintains a comparable performance to the expensive full-attention fine-tuned baseline.

| Model | Method | Length | Single-Doc | Multi-Doc | Summ. | Few-Shot | Code |
|--------------|---------|--------|------------|-----------|-------|----------|------|
| Qwen-2.5-7B | Full | 32K | 41.9 | 45.2 | 26.5 | 69.1 | 64.9 |
| | Full-FT | 32K | 42.7 | 46.1 | 26.7 | 67.6 | 66.3 |
| | Ours | 32K | 42.5 | 45.8 | 26.8 | 67.4 | 66.4 |
| Qwen-2.5-14B | Full | 32K | 42.5 | 52.9 | 25.1 | 71.7 | 66.7 |
| | Full-FT | 32K | 43.9 | 50.5 | 27.1 | 68.8 | 67.1 |
| | Ours | 32K | 43.4 | 49.9 | 27.1 | 68.5 | 67.4 |

ing, resulting in inferior performance on these tasks. However, this problem should be mitigated by adjusting the composition of training data. We add 200 synthetic samples (100 for VT and 100 for CWE) with 20K maximum context length to the training data and fine-tune the model. The new model, denoted as “Ours+Synthetic FT”, achieves substantial improvements on both VT and CWE while preserving its competitive performances on other tasks. This observation further validates the effectiveness of our Activation Beacon: it can quickly learn the desired compression capability given a limited set of training data.

E EXPERIMENTS ON LARGER MODELS

We apply Activation Beacon on Qwen-2.5-7B and Qwen-2.5-14B to inspect its performance on larger models. The LongBench evaluation results (with a uniform x4 compression ratio) are shown in Table 8. It can be observed that Activation Beacon retains its effectiveness, holding comparable performance to the full-attention fine-tuned baseline.

Additionally, we report the training & inference efficiency of 14B models in Table 5 and Table 6, respectively. Activation Beacon significantly reduces the memory costs during training, enabling efficient training of large models at high speed. Besides, it stably accelerates the inference process while being much more memory-efficient than the full-attention baseline.